

ROC movies — a new generalization to a popular classic

Tilmann Gneiting^{1,2} and Eva–Maria Walz^{2,1}

¹Computational Statistics, Heidelberg Institute for Theoretical Studies, Heidelberg, Germany

²Institute for Stochastics, Karlsruhe Institute of Technology, Karlsruhe, Germany

March 29, 2022

Main Text

Abstract

Throughout science and technology, receiver operating characteristic (ROC) curves and associated area under the curve (AUC) measures constitute powerful tools for assessing the predictive abilities of features, markers and tests in binary classification problems. Despite its immense popularity, ROC analysis has been subject to a fundamental restriction, in that it applies to dichotomous (yes or no) outcomes only. We introduce ROC movies and universal ROC (UROC) curves that apply to just any ordinal or real-valued outcome, along with a new, asymmetric coefficient of predictive ability (CPA) measure. CPA equals the area under the UROC curve and admits appealing interpretations in terms of probabilities and rank based covariances. ROC movies, UROC curves and CPA nest and generalize the classical ROC curve and AUC, and are bound to supersede them in a wealth of applications.

Originating from signal processing and psychology, popularized in *Science* articles by Swets (1–2), and witnessing a surge of uses in machine learning (3–4), receiver operating characteristic or relative operating characteristic (ROC) curves and area under the ROC curve (AUC) measures (5) belong to the most widely used quantitative tools in science and technology (6). In a nutshell, the ROC curve quantifies the potential value of a real-valued feature, marker or test as a predictor of a binary outcome. To give an example, Fig. 1 illustrates the initial levels of two biomedical markers, serum albumin and serum bilirubin, in a Mayo Clinic trial on primary biliary cirrhosis (PBC), a chronic fatal disease of the liver. While patient records provide the duration of survival in days, traditional ROC analysis mandates the reduction of the outcome to a binary event, which here we take as survival beyond four years (7–9). Assuming that higher marker values are more indicative of survival, we can take any threshold value to predict survival if the marker exceeds the threshold, and non-survival otherwise. This type of binary predictor yields true positives, false positives (erroneous predictions of survival), true negatives, and false negatives (erroneous predictions of non-survival). The ROC curve is the piecewise linear curve that plots the true positive rate, or sensitivity, versus the false positive rate, or one minus the specificity, as the threshold for the predictor moves through all possible values.

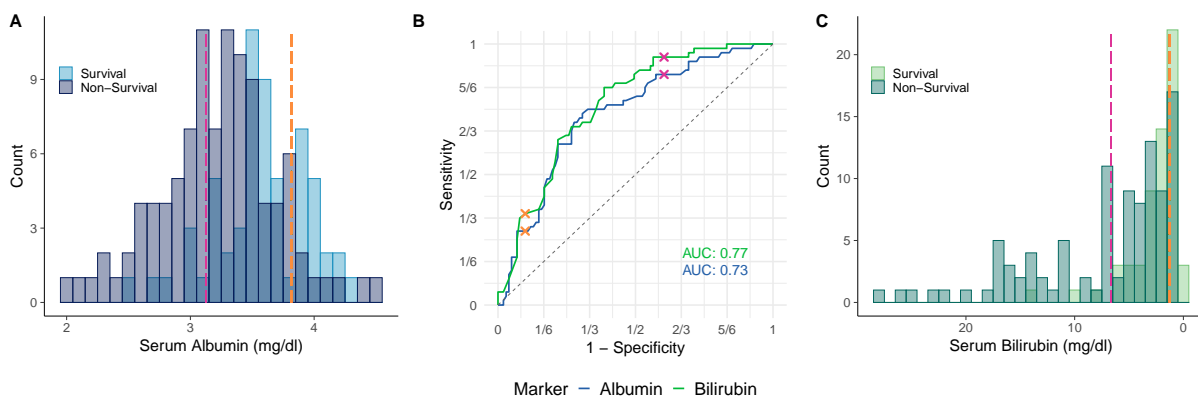


Figure 1: Traditional ROC curves for two biomedical markers, serum albumin and serum bilirubin, as predictors of patient survival beyond a threshold value of 1462 days (four years) in a Mayo Clinic trial. (A, C) Bar plots of marker levels conditional on survival or non-survival. The stronger shading results from overlap. For bilirubin, we reverse orientation, as is customary in the biomedical literature. (B) ROC curves and AUC values. The crosses correspond to binary predictors at the feature thresholds indicated in panels A and C, respectively.

ROC curves and AUC enjoy attractive properties (3–4, 10); e.g., they are purely rank based and invariant under strictly increasing transformations of the feature values. AUC is a positively oriented measure of discrimination ability that relates linearly to Somers’ D , a classical asymmetric coefficient of association (11), and admits an appealing interpretation as the probability that a feature value for a positive case is larger than a feature value for a negative case. In other words, AUC equals the probability that randomly drawn pairs of feature values and binary outcomes are concordant.

Despite its popularity, ROC analysis has been subject to a fundamental shortcoming, namely, the restriction to binary outcomes. Real-valued outcomes are ubiquitous in scientific practice, and researchers have been forced to artificially make them binary if the tools of ROC analysis are to be applied. In this light, researchers have been seeking generalizations of ROC analysis that apply to just any type of ordinal or real-valued outcome in natural ways. Still, notwithstanding decades of scientific endeavor, a satisfying generalization has been elusive (12–13). In machine learning, the originative construction of Hernández-Orallo (12) lacks a fundamental property of a generalization, in that it fails to reduce to the traditional ROC curve if the outcome is binary. In the biostatistical literature, researchers have studied time-dependent ROC curves (14–16), which can be understood as ingenious special types of ROC movies, but the discussion has been restricted to survival data, where matters are complicated due to censoring, and meaningful ways of averaging traditional ROC curves have not been found (16–20).

Here we propose a powerful generalization of ROC analysis, which overcomes all extant shortcomings, and introduce novel data analytic tools in the form of the ROC movie, the universal ROC (UROC) curve, and an associated asymmetric, rank based coefficient of predictive

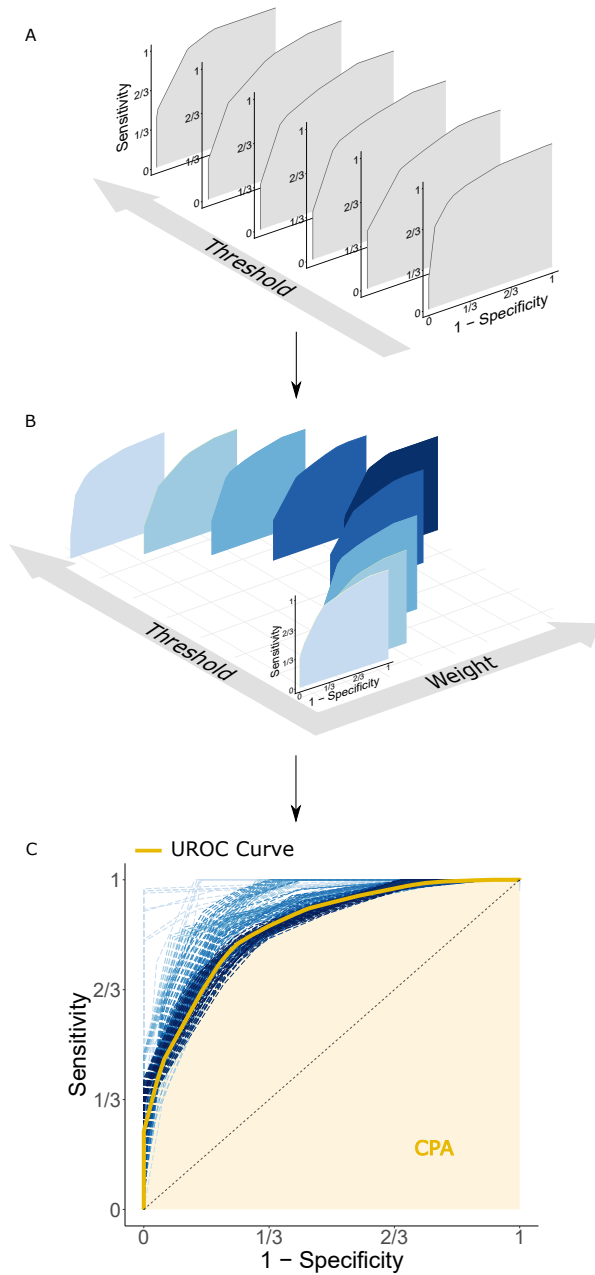


Figure 2: Construction of the ROC movie, universal ROC (UROC) curve and coefficient of predictive ability (CPA). **(A)** The ROC movie comprises the traditional ROC curves for binary events that correspond to successively higher threshold values for the real-valued outcome. **(B)** The individual ROC curves within the ROC movie are assigned judiciously chosen weights, as represented by the shading, where darker colors indicate higher weights. **(C)** The UROC curve arises as the respectively weighted average (21); CPA equals the area under the UROC curve and admits appealing alternative interpretations (24).

ability (CPA) measure — tools that apply to just any linearly ordered outcome, including both binary, ordinal, mixed discrete-continuous and continuous variables. Figure 2 provides a graphical overview; detailed and mathematically rigorous statements and proofs can be found in Section 3 of the Supplementary Text. In a nutshell, the ROC movie comprises the sequence of the traditional, static ROC curves as the linearly ordered outcome is converted to a binary variable at successively higher thresholds. The UROC curve is a weighted average of the individual ROC curves that constitute the ROC movie, with weights that depend on the class configuration, as induced by the unique values of the outcome, in judiciously predicated, well-defined ways (21).

CPA is a weighted average of the individual AUC values in the very same way that the UROC curve is a weighted average of the individual ROC curves that comprise the ROC movie (21). Hence, CPA equals the area under the UROC curve. In stark contrast to customarily used measures of bivariate association and dependence (22–23), CPA is asymmetric, i.e., in general, its value changes if the roles of the feature and the outcome are transposed. Thus, the new measure is directed and quantifies predictive ability. CPA attains values between 0 and 1, admits an interpretation as a weighted probability of concordance, and relates linearly to a rank based covariance between the class of the outcome and the rank of the feature (24). In particular, CPA reduces to AUC if the outcomes are binary, and relates linearly to Spearman’s rank correlation coefficient (25) if the outcomes are pairwise distinct, just as AUC relates linearly to Somers’ D . In this way, CPA nests and bridges AUC, Somers’ D and Spearman’s coefficient.

ROC movies, UROC curves and CPA are purely rank based and, therefore, they are invariant under strictly increasing transformations of feature and outcome values. As an immediate consequence, generalized ROC analysis serves to quantify the discrimination ability or *potential* predictive ability — as opposed to *actual* value — of a feature, marker or test, as is well known in the nested case of ROC curves and AUC (26, page 416). For a perfect feature, $CPA = 1$; for a feature that is independent of the outcome, $CPA = \frac{1}{2}$.

In Fig. 3 we illustrate ROC movies, UROC curves and CPA on the primary biliary cirrhosis (PBC) data considered earlier, where the outcome of interest is duration of survival in days. The CPA values for serum albumin and serum bilirubin are .73 and .77, respectively, and contrary to the ranking in Fig. 1, where bilirubin was deemed superior, based on outcomes that were artificially made binary. Our new tools free researchers from the need to binarize, and still they allow for an assessment at the binary level, if desired. For example, the ROC curves and AUC values from Fig. 1 appear in the ROC movie at a threshold value of 1462 days. In line with current uses of AUC in a gamut of applied settings, CPA is particularly well suited to the purposes of feature screening and variable selection in statistical and machine learning models (27). Here, AUC and CPA demonstrate that both albumin and bilirubin contribute to prognostic models for survival (7–8).

Another usage is in performance monitoring and record keeping for scientific, administrative and other purposes, as illustrated in Fig. 4, where we draw on CPA to assess progress in numerical weather prediction (NWP, 28–30). Specifically, we consider forecasts of temperature, wind speed and precipitation over Europe at lead times from a single to five days ahead from

Figure 3: ROC movie, UROC curve and CPA for two biomedical markers, serum albumin and serum bilirubin, as predictors of patient survival (in days) in a Mayo Clinic trial. The ROC movie shows the traditional ROC curves for binary events that correspond to patient survival beyond successively higher thresholds. The numbers at upper left show the current value of the threshold in days, at upper middle the respective relative weight, and at bottom right the AUC values (21). The threshold value of 1462 days recovers the traditional ROC curves in Fig. 1. The movie ends in a static screen with the UROC curves and CPA values for the two markers.

the high-resolution run operated by the European Centre for Medium-Range Weather Forecasts (ECMWF, 31–32), which is generally considered the leading global NWP model. The highest CPA values are seen for temperature, followed by wind speed and precipitation. Not surprisingly, the shorter the forecast lead time, the higher CPA. For all variables and lead times considered, CPA improves over time, attesting to steady progress in NWP.

To summarize, we have addressed a long-standing challenge in data analytics, by introducing a set of tools — comprising ROC movies, UROC curves and CPA — for generalized ROC analysis, thereby freeing researchers from the need to artificially binarize real-valued outcomes. In view of the advent of dynamic graphics in mainstream scientific publishing, we contend that ROC movies, UROC curves and CPA are bound to supersede traditional ROC curves and AUC in a wealth of applications. Open source code for their implementation in the R language and environment for statistical computing (33) is available on GitHub (34).

References and Notes

1. J. A. Swets, The relative operating characteristic in psychology. *Science* **182**, 990–1000 (1973).

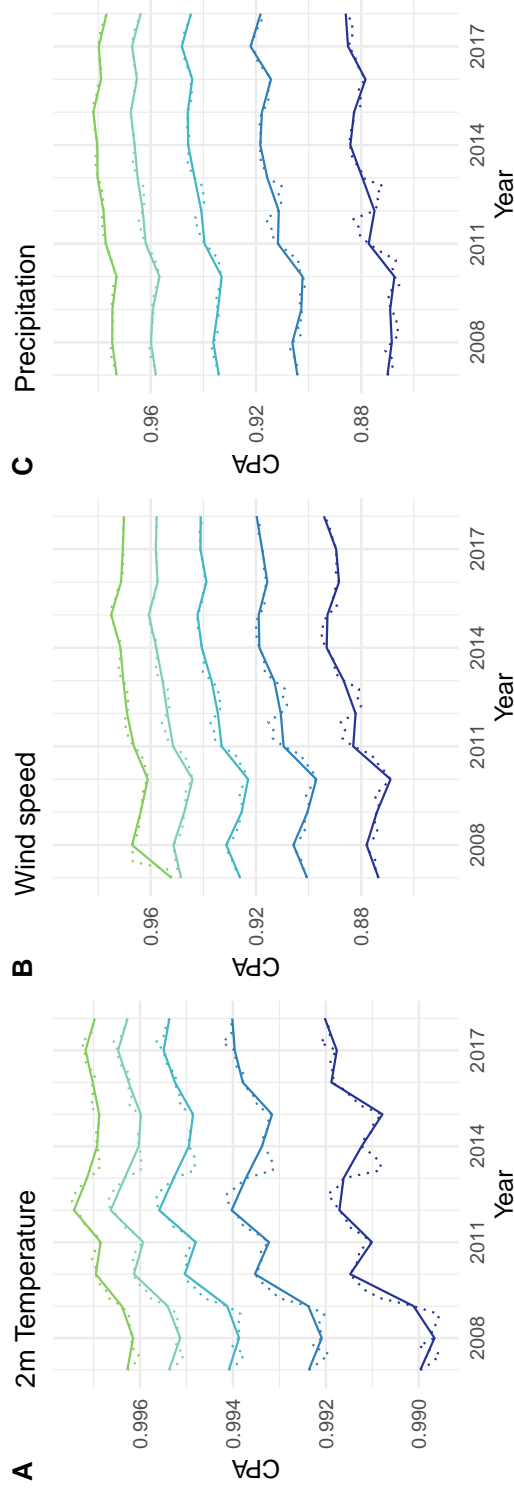


Figure 4: Temporal evolution of CPA for forecasts of (A) surface (2-meter) temperature, (B) wind speed and (C) 24-hour precipitation accumulation from the European Centre for Medium-Range Weather Forecasts (ECMWF) high-resolution model at lead times from one to five days. The CPA values refer to a domain that covers Europe and twelve months periods that correspond to January–December (solid and dotted lines), April–March, July–June and October–September (dotted lines only), based on gridded forecast and observational data from January 2007 through December 2018.

2. J. A. Swets, Measuring the accuracy of diagnostic systems. *Science* **240**, 1285–1293 (1988).
3. T. Fawcett, An introduction to ROC analysis. *Pattern Recognit. Lett.* **27**, 861–874 (2006).
4. P. A. Flach, ROC analysis, in *Encyclopedia of Machine Learning and Data Mining*, C. Sammut, G. I. Webb, eds. (Springer, 2016).
5. J. A. Hanley, B. J. McNeil, The meaning and use of the area under a receiver operating characteristic (ROC) curve. *Radiology* **143**, 29–36 (1982)
6. A Web of Science topic search for the terms “receiver operating characteristic” or “ROC” yields well over 12,000 scientific papers published in 2018 alone.
7. E. R. Dickson, P. M. Grambsch, T. R. Fleming, L. D. Fischer, A. Langworthy, Prognosis in primary biliary cirrhosis: Model for decision making. *Hepatology* **10**, 1–7 (1989).
8. T. R. Fleming, D. P. Harrington. *Counting Processes and Survival Analysis* (New York, Wiley, 1991).
9. For the purposes of this illustration, we ignore issues caused by censoring and consider non-censored patients only, so all survival times are known. See Section 4.1 of the Supplementary Text for details.
10. M. S. Pepe, *The Statistical Evaluation of Medical Tests for Classification and Prediction* (New York, Oxford University Press, 2003).
11. R. H. Somers, A new asymmetric measure of association for ordinal variables. *Am. Sociol. Rev.* **27**, 799–811 (1962).
12. J. Hernández-Orallo, ROC curves for regression. *Pattern Recognit.* **46**, 3395–3411 (2013).
13. Hernández-Orallo (13, page 3395) notes that “there is no such a thing as the ‘canonical’ adaptation of ROC analysis in regression” and “it is even questionable whether a similar graphical representation of ROC curves [...] can even be figured out.”
14. R. Etzioni, M. Pepe, G. Longton, C. Hu, G. Goodman, Incorporating the time dimension in receiver operating characteristic curves: A study of prostate cancer. *Med. Decis. Mak.* **19**, 242–251 (1999).
15. P. J. Heagerty, T. Lumley, M. S. Pepe, Time-dependent ROC curves for censored survival data and a diagnostic marker. *Biometrics* **56**, 337–344 (2000).
16. P. J. Heagerty, Y. Zheng, Survival model predictive accuracy and ROC curves. *Biometrics* **61**, 92–105 (2005).

17. S. Rosset, C. Perlich, B. Zadrozny, Ranking-based evaluation of regression models. *IEEE ICDM'05* (2005).
18. M. J. Pencina, R. B. D'Agostino, Overall C as a measure of discrimination in survival analysis: Model specific population value and confidence interval estimation. *Stat. Med.* **22**, 2109–2123 (2004).
19. S. J. Mason, A. P. Weigel, A generic forecast verification framework for administrative purposes. *Mon. Wea. Rev.* **137**, 331–349 (2009).
20. The displays in Figs. 2 and 3 of Etzioni et al. (14), Fig. 2 of Heagerty et al. (15) and Figs. 1(a) and 3 of Heagerty and Zheng (16) can be interpreted as (statistically fitted) partial (static) versions of ROC movies in the setting of survival data. However, Heagerty and Zheng (16, page 95) note that “methods have not been proposed for meaningfully averaging the time-specific” AUC values. In a general regression setting, Rosset et al. (17) propose plots of threshold-specific AUC values. Pencina et al. (18) and Mason and Weigel (19) discuss analogues of AUC that relate linearly to Kendall’s rank correlation coefficient if the outcomes are real-valued, much in line with the definition of Somers’ D in the general case of ordinal outcomes (11). For details, see Section 3.4.1 in the Supplementary Text.
21. For formal introductions of the UROC curve and CPA see Definitions 3.2 and 3.3 in the Supplementary Text.
22. D. N. Reshef, Y. A. Reshef, H. K. Finucane, S. R. Grossman, G. McVean, P. J. Turnbaugh, E. S. Lander, M. Mitzenmacher, P. C. Sabeti, Detecting novel associations in large data sets. *Science* **334**, 1518–1524 (2011).
23. L. Weihs, M. Drton, N. Meinshausen, Symmetric rank covariances: A generalized framework for nonparametric measures of dependence. *Biometrika* **105**, 547–562 (2018).
24. For formal statements and proofs of the claims in this paragraph see Theorems 3.4–3.7 in the Supplementary Text. The representation in terms of rank based covariances allows the efficient computation of CPA, as we discuss in Section 3.5 of the Supplementary Text.
25. C. Spearman, The proof and measurement of association between two things. *Am. J. Psychol.* **15**, 72–101 (1904).
26. D. S. Wilks, *Statistical Methods in the Atmospheric Sciences*, fourth edition (Elsevier, 2019).
27. I. Guyon, A. Elisseeff, An introduction to variable and feature selection. *J. Mach. Learn. Res.* **3**, 1157–1182 (2003).

28. P. Bauer, A. Thorpe, G. Brunet, The quiet revolution of numerical weather prediction. *Nature* **525**, 47–55 (2015).
29. R. B. Alley, K. A. Emanuel, F. Zhang, Advances in weather prediction. *Science* **363**, 342–344 (2019).
30. Z. Ben Bouallègue, L. Magnusson, T. Haiden, D. S. Richardson, Monitoring trends in ensemble forecast performance focusing on surface variables and high-impact events. *Q. J. Roy. Meteorol. Soc.* **145**, 1741–1755 (2019).
31. ECMWF Directorate, Describing ECMWF’s forecasts and forecasting system. *ECMWF Newsl.* **133**, 11–13 (2012).
32. For details and additional analyses see Section 4.2 of the Supplementary Text.
33. R Core Team, R: A language and environment for statistical computing. R Foundation for Statistical Computing, Vienna, Austria, <https://www.r-project.org/> (2019).
34. E.-M. Walz, Replication materials and R code for ROC movies, UROC curves and CPA, https://github.com/evwalz/CPA_Example_NWP; <https://github.com/evwalz/uroc> (2019).

Acknowledgments

We thank Zied Ben Bouallègue, Timo Dimitriadis, Andreas Eberl, Dominic Edelmann, Andreas Fink, Peter Knippertz, Sebastian Lerch, Marlon Maranan, Florian Pappenberger, Johannes Resin, Peter Sanders, David Richardson, Philipp Zschenderlein and seminar participants at the European Centre for Medium-Range Weather Forecasts (ECMWF) and International Symposium on Forecasting (ISF) for advice, discussion and encouragement. This work has been supported by the Klaus Tschira Foundation and by the Deutsche Forschungsgemeinschaft (DFG, German Research Foundation) – Project-ID 257899354 – TRR 165. Tilmann Gneiting furthermore acknowledges travel support via the ECMWF Fellowship programme.

Supplementary materials

Supplementary Text

Figures **5** to **8**

Table **1**

References (35–50)

ROC movies — a new generalization to a popular classic

Tilmann Gneiting^{1,2} and Eva–Maria Walz^{2,1}

¹Computational Statistics, Heidelberg Institute for Theoretical Studies, Heidelberg, Germany

²Institute for Stochastics, Karlsruhe Institute of Technology, Karlsruhe, Germany

March 29, 2022

Supplementary Text

Abstract

Aimed at a broad scientific audience, our nontechnical main article introduces receiver operating characteristic (ROC) movies and universal ROC (UROC) curves that apply to general real-valued outcomes, along with a new, rank based coefficient of predictive ability (CPA) measure. CPA equals the area under the UROC curve and relates linearly to a ratio of rank based covariances, which nests both Somers' D and Spearman's rank correlation coefficient. In this supplement, we provide a technical account of the mathematical and statistical developments, report on a brief simulation study and give details for the data examples in the main text.

1 Introduction

We begin this supplement with a brief review of classical receiver operating characteristic (ROC) analysis for dichotomous (binary) outcomes in Section 2. The key technical development is in Section 3.1, where we introduce and study ROC movies, universal ROC (UROC) curves and an asymmetric, rank based coefficient of predictive ability (CPA), which equals the area under the UROC curve. In Section 4 we give details and additional results for the liver disease survival and numerical weather prediction (NWP) examples in the main text.

2 Receiver operating characteristic (ROC) curves and area under the curve (AUC) for binary outcomes

In order to introduce ROC movies, UROC curves and CPA, it is essential that we review the classical case of ROC analysis for binary outcomes (*1–5*, *10*).

2.1 Binary setting

Throughout this section we consider bivariate data of the form

$$(x_1, y_1), \dots, (x_n, y_n) \in \mathbb{R} \times \{0, 1\}, \quad (2.1)$$

where $x_i \in \mathbb{R}$ is a real-valued¹ feature, marker or covariate value, and $y_i \in \{0, 1\}$ is a binary outcome, for $i = 1, \dots, n$. Following the extant literature, we refer to $y = 1$ as the positive outcome and to $y = 0$ as the negative outcome, and we assume that higher values of the feature are indicative of stronger support for the positive outcome. Throughout we assume that there is at least one index $i \in \{1, \dots, n\}$ with $y_i = 0$, and a further index $j \in \{1, \dots, n\}$ with $y_j = 1$.

2.2 Receiver operating characteristic (ROC) curves

We can use any threshold value $x \in \mathbb{R}$ to obtain a hard classifier, by predicting a positive outcome for a feature value $> x$, and predicting a negative outcome for a feature value $\leq x$. If we compare to the actual outcome, four possibilities arise. True positive and true negative cases correspond to correctly classified instances from class 1 and class 0. Similarly, false positive and false negative cases are misclassified instances from class 1 and class 0, respectively.

Considering the data (2.1), we obtain the respective *true positive rate*, *hit rate* or *sensitivity* (se),

$$\text{se}(x) = \frac{\frac{1}{n} \sum_{i=1}^n \mathbb{1}\{x_i > x, y_i = 1\}}{\frac{1}{n} \sum_{i=1}^n \mathbb{1}\{y_i = 1\}},$$

and the *false negative rate*, *false alarm rate* or one minus the *specificity* (sp),

$$1 - \text{sp}(x) = \frac{\frac{1}{n} \sum_{i=1}^n \mathbb{1}\{x_i > x, y_i = 0\}}{\frac{1}{n} \sum_{i=1}^n \mathbb{1}\{y_i = 0\}},$$

at the threshold value $x \in \mathbb{R}$, where the indicator $\mathbb{1}\{A\}$ equals one if the event A is true and zero otherwise.

Evidently, it suffices to consider threshold values x equal to any of the unique values of x_1, \dots, x_n or some $x_0 < x_1$. For every x of this form, we obtain a point

$$(1 - \text{sp}(x), \text{se}(x))$$

in the unit square. Linear interpolation of the respective discrete point set results in a piecewise linear curve from $(0, 0)$ to $(1, 1)$ that is called the *receiver operating characteristic (ROC) curve*. For a mathematically oriented, detailed discussion of the construction see Section 2 of Gneiting and Vogel (36).

¹Without loss of generality, we assume that the feature is real-valued. However, as all results and techniques discussed are rank based, they carry through for linearly ordered features. For generalizations of ROC analysis to categorical outcomes that cannot be linearly ordered see Hand and Till (35) and Section 9 of Fawcett (3).

2.3 Area under the curve (AUC)

The area under the ROC curve is a widely used measure of the predictive potential of a feature and generally referred to as the *area under the curve* (AUC).

In what follows, a well-known interpretation of AUC in terms of probabilities will be useful. To this end, we define the function

$$s(x, x') = \mathbb{1}\{x < x'\} + \frac{1}{2}\mathbb{1}\{x = x'\}, \quad (2.2)$$

where $x, x' \in \mathbb{R}$. For subsequent use, note that if x and x' are ranked within a list, and ties are resolved by assigning equal ranks within tied groups, then $s(x, x') = s(\text{rk}(x), \text{rk}(x'))$.

We now change notation and refer to the feature values in class $i \in \{0, 1\}$ as x_{ik} for $k = 1, \dots, n_i$, where $n_0 = \sum_{i=1}^n \mathbb{1}\{y_i = 0\}$ and $n_1 = \sum_{i=1}^n \mathbb{1}\{y_i = 1\}$, respectively. Thus, we have rewritten (2.1) as

$$(x_{01}, 0), \dots, (x_{0n_0}, 0), (x_{11}, 1), \dots, (x_{1n_1}, 1) \in \mathbb{R} \times \{0, 1\}. \quad (2.3)$$

Using the new notation, Result 4.10 of Pepe (10) states that

$$\text{AUC} = \frac{1}{n_0 n_1} \sum_{i=1}^{n_0} \sum_{j=1}^{n_1} s(x_{0i}, x_{1j}). \quad (2.4)$$

In words, AUC equals the probability that under random sampling a feature value from a positive instance is greater than a feature value from a negative instance, with any ties resolved at random. Expressed differently, AUC equals the tie-adjusted probability of concordance in feature–outcome pairs, where we define instances $(x, y) \in \mathbb{R}^2$ and $(x', y') \in \mathbb{R}^2$ with $y \neq y'$ to be *concordant* if either $x > x'$ and $y > y'$, or $x < x'$ and $y < y'$. Similarly, instances (x, y) and (x', y') with $y \neq y'$ are *discordant* if either $x > x'$ and $y < y'$, or $x < x'$ and $y > y'$.

Further investigation reveals a close connection to Somers' D , a classical measure of ordinal association (11). This measure is defined as

$$D = \frac{n_c - n_d}{n_0 n_1},$$

where $n_0 n_1$ is the total number of pairs with distinct outcomes that arise from the data in (2.3), n_c is the number of concordant pairs, and n_d is the number of discordant pairs. Finally, let n_e be the number of pairs for which the feature values are equal. The relationship (2.4) yields

$$\text{AUC} = \frac{n_c}{n_0 n_1} + \frac{1}{2} \frac{n_e}{n_0 n_1},$$

and as $n_0 n_1 = n_c + n_d + n_e$, it follows that

$$\text{AUC} = \frac{1}{2} (D + 1) \quad (2.5)$$

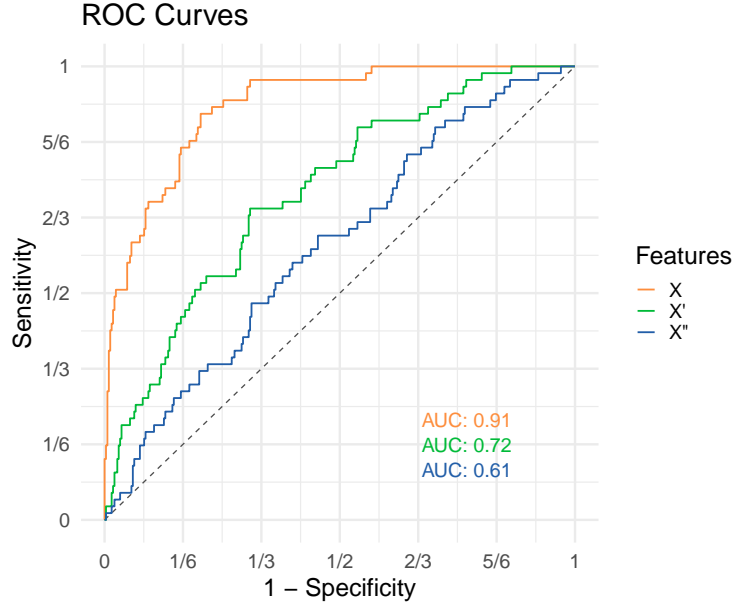


Figure 5: Traditional ROC curves and AUC values for the features X , X' and X'' as predictors of the binary outcome $Y_1 = \mathbb{1}\{Y \geq 1\}$ in the simulation example of Section 2.3, based on a sample of size $n = 400$.

relates linearly to Somers' D .

To give an example, suppose that the real-valued outcome Y and the features X , X' and X'' are jointly Gaussian. Specifically, we assume that the joint distribution of (Y, X, X', X'') is multivariate normal with covariance matrix

$$\begin{pmatrix} 1 & 0.8 & 0.5 & 0.2 \\ 0.8 & 1 & 0.8 & 0.5 \\ 0.5 & 0.8 & 1 & 0.8 \\ 0.2 & 0.5 & 0.8 & 1 \end{pmatrix}. \tag{2.6}$$

In order to apply classical ROC analysis, the real-valued outcome Y needs to be converted to a binary variable, namely, an event of the type $Y_\theta = \mathbb{1}\{Y \geq \theta\}$ of Y being greater than or equal to a certain threshold value θ . Figure 5 shows ROC curves for the features X , X' and X'' as a predictor of the induced binary variable Y_1 , based on a sample of size $n = 400$. The AUC values for X , X' and X'' as a predictor of Y_1 are .91, .72 and .61, respectively. While the choice of the threshold value $\theta = 1$ is arbitrary and artificial, as is often the case in practice, its specification is mandated by the limitations of classical ROC analysis.

2.4 Summary

Despite being applicable to binary outcomes only, classical ROC analysis has been an attractive and immensely popular procedure, for reasons as follows:

- (1) The ROC curve and AUC are straightforward to compute and interpret, in the (rough) sense of *the larger the better*.
- (2) AUC attains values between 0 and 1 and relates linearly to Somers' D . For a perfect feature, $\text{AUC} = 1$ and $D = 1$; for a feature that is independent of the binary outcome, $\text{AUC} = \frac{1}{2}$ und $D = 0$.
- (3) The numerical value of AUC admits an interpretation as the probability of concordance for feature–outcome pairs.
- (4) The ROC curve and AUC are purely rank based and, therefore, invariant under strictly increasing transformations. Specifically, if $\phi : \mathbb{R} \rightarrow \mathbb{R}$ is a strictly increasing function, then the ROC curve and AUC computed from

$$(\phi(x_1), y_1), \dots, (\phi(x_n), y_n) \in \mathbb{R} \times \{0, 1\}. \quad (2.7)$$

are the same as the ROC curve and AUC computed from (2.1).

As an immediate consequence of property, ROC curves and AUC assess the discrimination ability or *potential* predictive ability of a feature, marker or test (26). Distinctly different methods are called for if one seeks to evaluate a forecast's *actual* value in an applied setting.

3 ROC movies, universal ROC (UROC) curves and coefficient of predictive ability (CPA) for real-valued outcomes

As noted, traditional ROC analysis applies to binary outcomes only. Thus, researchers working with real-valued outcomes, and desiring to apply ROC analysis, need to convert and reduce to binary outcomes, by thresholding artificially at a cut-off value. The tools that we introduce now free researchers from this need.

3.1 General real-valued setting

Generalizing the binary setting in (2.1), we now consider bivariate data of the form

$$(x_1, y_1), \dots, (x_n, y_n) \in \mathbb{R} \times \mathbb{R}, \quad (3.1)$$

where x_i is a real-valued feature, marker or covariate value, and y_i is a real-valued outcome, for $i = 1, \dots, n$. Throughout we assume that there are at least two unique values among the outcomes y_1, \dots, y_n .

The crux of the subsequent development lies in a conversion to a sequence of binary problems. To this end, we let

$$z_1 < \cdots < z_m$$

denote the $m \leq n$ distinct order statistics of y_1, \dots, y_n , and we define

$$n_c = \sum_{i=1}^n \mathbb{1}\{y_i = z_c\}$$

as the number of instances among the outcomes y_1, \dots, y_n that equal z_c , for $c = 1, \dots, m$, so that $n_1 + \cdots + n_m = n$. We refer to the respective groups of instances as *classes*.

Next we transform the real-valued outcomes y_1, \dots, y_n into binary outcomes $\mathbb{1}\{y_1 \geq \theta\}, \dots, \mathbb{1}\{y_n \geq \theta\}$ relative to a threshold value $\theta \in \mathbb{R}$. Thus, instead of analysing the original problem in (3.1), we consider a series of binary problems. By construction, only values of θ equal to the distinct order statistics $z_2 < \cdots < z_m$ result in nontrivial, unique sets of binary outcomes. Therefore, we consider $m - 1$ derived classification problems with binary data of the form

$$(x_1, \mathbb{1}\{y_1 \geq z_{c+1}\}), \dots, (x_n, \mathbb{1}\{y_n \geq z_{c+1}\}) \in \mathbb{R} \times \{0, 1\}, \quad (3.2)$$

where $c = 1, \dots, m - 1$. As the derived problems are binary, all the tools of traditional ROC analysis apply.

In the remainder of the section we describe our generalization of ROC curves for binary data to ROC movies and universal ROC (UROC) curves for real-valued data. First, we argue that the $m - 1$ classical ROC curves for the derived data in (3.2) can be merged into a single dynamical display, to which we refer as a ROC movie (Definition 3.1). Then we define the UROC curve as a judiciously weighted average of the classical ROC curves of which the ROC movie is composed (Definition 3.2).

Finally, we introduce a general measure of potential predictive ability for features, termed the coefficient of predictive ability (CPA). CPA is a weighted average of the AUC values for the derived binary problems in the very same way that the UROC curve is a weighted average of the (classical) ROC curves that comprise the ROC movie. Hence, CPA equals the area under the UROC curve (Definition 3.3). Alternatively, CPA can be interpreted as a weighted probability of concordance (Theorem 3.4) or in terms of rank based covariances (Theorem 3.5). CPA reduces to AUC if the outcomes are binary, and relates linearly to Spearman's rank correlation coefficient if the outcomes are continuous (Theorems 3.6 and 3.7).

3.2 ROC movies

We consider the sequence of $m - 1$ classification problems for the derived binary data in (3.2). For $c = 1, \dots, m - 1$, we let ROC_c denote the associated ROC curve, and we let AUC_c be the respective AUC value.

Definition 3.1. For data of the form (3.1), the ROC movie is the sequence $(\text{ROC}_c)_{c=1, \dots, m-1}$ of the ROC curves for the induced binary data in (3.2).

Figure 6: ROC movies and UROC curves for the features X , X' and X'' as predictors of the real-valued outcome Y in the simulation example of Section 2.3, based on the same sample as in Fig. 5. In the ROC movies, the number at upper left shows the threshold under consideration, the number at upper center the relative weight $w_c / \max_{l=1, \dots, m-1} w_l$ from (3.4), and the numbers at bottom right the respective AUC values.

If the original problem is binary there are $m = 2$ classes only, and the ROC movie reduces to the classical ROC curve. In case the outcome attains $m \geq 3$ distinct values the ROC movie can be visualized by displaying the associated sequence of $m - 1$ ROC curves. In medical survival analysis, the outcomes y_1, \dots, y_n in data of the form (3.1) are survival times, and the analysis is frequently hampered by censoring, as patients drop out of studies. In this setting, Etzioni et al. (14) and Heagerty et al. (15) introduced the notion of time-dependent ROC curves, which are classical ROC curves for the binary indicator $\mathbb{1}\{y_i \geq t\}$ of survival through (follow-up) time t . If the survival times considered correspond to the unique values in y_1, \dots, y_n , the sequence of time-dependent ROC curves becomes a ROC movie in the sense of Definition 3.1.

We have implemented ROC movies, UROC curves and CPA within the `uroc` package for the statistical programming language R (33–34). The `animation` package of Xie (37) provides functionality for converting R images into a GIF animation, based on the external software `ImageMagick`. Returning to the example of Section 2.3, Fig. 6 compares the features X , X' and X'' as predictors of the real-valued outcome Y in a joint display of the three ROC movies and UROC curves, based on the same sample of size $n = 400$ as in Fig. 5. In the ROC movies, the threshold $z = 1.00$ recovers the traditional ROC curves in Fig. 5.

If the number $m \leq n$ of classes is small or modest, the generation of the ROC movie is straightforward. Adaptations might be required as m grows, and we tend to this question in Section 4.2.

3.3 Universal ROC (UROC) curves

Next we propose a simple and efficient way of subsuming a ROC movie for data of the form (3.1) into a single, static graphical display. As before, let $z_1 < \dots < z_m$ denote the distinct values of y_1, \dots, y_n , let $n_c = \sum_{i=1}^n \mathbb{1}\{y_i = z_c\}$, and let ROC_c denote the (classical) ROC curve associated with the binary problem in (3.2), for $c = 1, \dots, m - 1$.

By Theorem 5 of Gneiting and Vogel (36), there is a natural bijection between the class of the ROC curves and the class of the cumulative distribution functions (CDFs) of Borel probability measures on the unit interval. In particular, any ROC curve can be associated with a non-decreasing, right-continuous function $R : [0, 1] \rightarrow [0, 1]$ such that $R(0) = 0$ and $R(1) = 1$. Hence, any convex combination of the ROC curves $\text{ROC}_1, \dots, \text{ROC}_{m-1}$ can also be associated with a non-decreasing, right-continuous function on the unit interval. It is in this sense that we define the following; in a nutshell, the UROC curve averages the traditional ROC curves of which the ROC movie is composed.

Definition 3.2. For data of the form (3.1), the *universal receiver operating characteristic* (UROC) curve is the curve associated with the function

$$\sum_{c=1}^{m-1} w_c \text{ROC}_c \quad (3.3)$$

on the unit interval, with weights

$$w_c = \left(\sum_{i=1}^c n_i \sum_{i=c+1}^m n_i \right) / \left(\sum_{i=1}^{m-1} \sum_{j=i+1}^m (j-i) n_i n_j \right) \quad (3.4)$$

for $c = 1, \dots, m - 1$.

Importantly, the weights in (3.4) depend on the data in (3.1) via the outcomes y_1, \dots, y_n only. Thus, they are independent of the feature values and can be used meaningfully in order to compare and rank features. Their specific choice is justified in Theorems 3.4 and 3.5 below. Clearly, the weights are nonnegative and sum to one. If $m = n$ then $n_1 = \dots = n_m = 1$, and (3.4) reduces to

$$w_c = 6 \frac{c(n-c)}{n(n^2-1)} \quad \text{for } c = 1, \dots, n-1; \quad (3.5)$$

so the weights are quadratic in the rank c and symmetric about the inner most rank(s), at which they attain a maximum. As we will see, our choice of weights has the effect that in this setting the area under the UROC curve, to which we refer as a general coefficient of predictive ability (CPA), relates linearly to Spearman's rank correlation coefficient, in the same way that AUC relates linearly to Somers' D .

In Fig. 6 the UROC curves appear in the final static screen, subsequent to the ROC movies. Within each ROC movie, the individual frames show the ROC curve ROC_c for the feature considered. Furthermore, we display the threshold z_c , the *relative* weight from (3.4) (the actual

weight normalized to the unit interval, i.e., we show $w_c / \max_{l=1, \dots, m-1} w_l$, and AUC_c , respectively, for $c = 1, \dots, m-1$. Once more we emphasize that the use of ROC movies, UROC curves and CPA frees researchers from the need to select — typically, arbitrary — threshold values and binarize, as mandated by classical ROC analysis.

Of course, if specific threshold values are of particular substantive interest, the respective ROC curves can be extracted from the ROC movie. Furthermore, in comparing competing features relative to particular thresholds, weightings other than (3.4) can be considered, and it can be useful to plot the respective values of AUC_c versus the threshold value z_c . Displays of this type have been introduced and studied by Rosset et al. (17).

3.4 Coefficient of predictive ability (CPA)

We proceed to define the coefficient of predictive ability (CPA) as a general measure of potential predictive ability.

Definition 3.3. For data of the form (3.1) and weights w_1, \dots, w_{m-1} as in (3.4), the *coefficient of predictive ability* (CPA) is defined as

$$\text{CPA} = \sum_{c=1}^{m-1} w_c \text{AUC}_c. \quad (3.6)$$

In words, CPA equals the area under the UROC curve.

Importantly, ROC movies, UROC curves and CPA satisfy a fundamental requirement on any generalization of ROC curves and AUC, in that they reduce to the classical notions when applied to a binary problem, whence $m = 2$ in (3.3) and (3.6), respectively.

3.4.1 Interpretation as a weighted probability

We now express CPA in terms of pairwise comparisons via the function s in (2.2). To this end, we usefully change notation for the data in (3.1) and refer to the feature values in class $c \in \{1, \dots, m\}$ as x_{ck} , for $k = 1, \dots, n_l$. Thus, we rewrite (3.1) as

$$(x_{11}, z_1), \dots, (x_{1n_1}, z_1), \dots, (x_{m1}, z_m), \dots, (x_{mn_m}, z_m) \in \mathbb{R} \times \mathbb{R}, \quad (3.7)$$

where $z_1 < \dots < z_m$ are the unique order statistics of y_1, \dots, y_n and $n_c = \sum_{i=1}^n \mathbb{1}\{y_i = z_c\}$, for $c = 1, \dots, m$.

Theorem 3.4. For data of the form (3.7),

$$\text{CPA} = \frac{\sum_{i=1}^{m-1} \sum_{j=i+1}^m \sum_{k=1}^{n_i} \sum_{l=1}^{n_j} (j-i) s(x_{ik}, x_{jl})}{\sum_{i=1}^{m-1} \sum_{j=i+1}^m (j-i) n_i n_j}. \quad (3.8)$$

Proof. By (2.4), the individual AUC values satisfy

$$\text{AUC}_c = \frac{1}{\sum_{i=1}^c n_i \sum_{i=c+1}^m n_i} \sum_{i=1}^c \sum_{j=c+1}^m \sum_{k=1}^{n_i} \sum_{l=1}^{n_j} s(x_{ik}, x_{jl})$$

for $c = 1, \dots, m - 1$. In view of (3.4) and (3.6), summation yields

$$\begin{aligned} \text{CPA} &= \sum_{c=1}^{m-1} w_c \text{AUC}_c \\ &= \frac{\sum_{c=1}^{m-1} \sum_{i=1}^c \sum_{j=c+1}^m \sum_{k=1}^{n_i} \sum_{l=1}^{n_j} s(x_{ik}, x_{jl})}{\sum_{i=1}^{m-1} \sum_{j=i+1}^m (j-i) n_i n_j} \\ &= \frac{\sum_{i=1}^{m-1} \sum_{j=i+1}^m \sum_{k=1}^{n_i} \sum_{l=1}^{n_j} (j-i) s(x_{ik}, x_{jl})}{\sum_{i=1}^{m-1} \sum_{j=i+1}^m (j-i) n_i n_j}, \end{aligned}$$

as claimed. \square

Thus, CPA is based on pairwise comparisons of feature values, counting the number of concordant pairs in (3.7), adjusting to a count of $\frac{1}{2}$ if feature values are tied, and weighting a pair's contribution by a class based distance, $j - i$, between the respective outcomes, $z_j > z_i$. In other words, CPA equals a weighted probability of concordance, with weights that grow linearly in the class based distance between outcomes.

The specific form of CPA in (3.8) invites comparison to a widely used measure of discrimination in biomedical applications, namely, the *C index* (18, 38–39)

$$C = \frac{\sum_{i=1}^{m-1} \sum_{j=i+1}^m \sum_{k=1}^{n_i} \sum_{l=1}^{n_j} s(x_{ik}, x_{jl})}{\sum_{i=1}^{m-1} \sum_{j=i+1}^m n_i n_j}. \quad (3.9)$$

If the outcomes are binary, both the C index and CPA reduce to AUC. While CPA can be interpreted as a weighted probability of concordance, C admits an interpretation as an unweighted probability, whence Mason and Weigel (19) recommend its use for administrative purposes. However, the weighting in (3.8) appears to be more meaningful, as concordances between feature–outcome pairs with outcomes that are far apart are bound to be of greater practical relevance than concordances between pairs with alike outcomes. While CPA admits the appealing, equivalent interpretation (3.6) in terms of binary AUC values and the area under the UROC curve, relationships of this type are unavailable for the C index.

Subject to conditions, the C index relates linearly to Kendall's rank correlation coefficient (11, 18–19). In Section 3.4.3 we demonstrate the same type of relationship for CPA and Spearman's rank correlation coefficient, thereby resolving a problem raised by Heagerty and Zheng (16, page 95). Just as the C index bridges and generalizes AUC and Kendall's coefficient, CPA bridges and nests AUC and Spearman's coefficient, with the added benefit of appealing interpretations in terms of the area under the UROC curve and rank based covariances.

3.4.2 Representation in terms of covariances

The key result in this section represents CPA in terms of the covariance between the class of the outcome and the mid rank of the feature, relative to the covariance between the class of the outcome and the mid rank of the outcome itself.

The mid rank method handles ties by assigning the arithmetic average of the ranks involved (40–41). For instance, if the third to seventh positions in a list are tied, their shared *mid rank* is $\frac{1}{5}(3+4+5+6+7) = 5$. This approach treats equal values alike and guarantees that the sum of the ranks in any tied group is unchanged from the case of no ties. As before, if $y_i = z_j$, where $z_1 < \dots < z_m$ are the unique order statistics of y_1, \dots, y_n in (3.1), we say that the *class* of y_i is j . In brief, we express this as $\text{cl}(y_i) = j$. Similarly, we refer to the mid rank of x_i within x_1, \dots, x_n as $\overline{\text{rk}}(x_i)$.

Theorem 3.5. *Let the random vector (X, Y) be drawn from the empirical distribution of the data in (3.1) or (3.7). Then*

$$\text{CPA} = \frac{1}{2} \left(\frac{\text{cov}(\text{cl}(Y), \overline{\text{rk}}(X))}{\text{cov}(\text{cl}(Y), \overline{\text{rk}}(Y))} + 1 \right). \quad (3.10)$$

Proof. Suppose that the law of the random vector (X, Y) is the empirical distribution of the data in (3.1). Based on the equivalent representation in (3.7), we find that

$$\frac{\text{cov}(\text{cl}(Y), \overline{\text{rk}}(X))}{\text{cov}(\text{cl}(Y), \overline{\text{rk}}(Y))} = \frac{\sum_{i=1}^m \sum_{k=1}^{n_i} i \overline{\text{rk}}(x_{ik}) - \frac{1}{2}(n+1) \sum_{i=1}^m i n_i}{\sum_{i=1}^m i n_i \left(\sum_{j=0}^{i-1} n_j + \frac{1}{2}(n_i + 1) \right) - \frac{1}{2}(n+1) \sum_{i=1}^m i n_i},$$

where $n_0 = 0$. Consequently, we can rewrite (3.10) as

$$\text{CPA} = \frac{\sum_{i=1}^m \sum_{k=1}^{n_i} i \overline{\text{rk}}(x_{ik}) + \sum_{i=1}^m i n_i \left(\sum_{j=0}^{i-1} n_j + \frac{1}{2} n_i - n - \frac{1}{2} \right)}{\sum_{i=1}^m i n_i \left(2 \sum_{j=0}^{i-1} n_j + n_i - n \right)}. \quad (3.11)$$

We proceed to demonstrate that the numerator and denominator in (3.8) equal the numerator and denominator in (3.11), respectively. To this end, we first compare feature values within classes and note that

$$\sum_{i=1}^m \sum_{k=1}^{n_i} \sum_{l=1}^{n_i} i s(x_{il}, x_{ik}) = \sum_{i=1}^m i \sum_{k=1}^{n_i} \left(n_i - k + \frac{1}{2} \right) = \frac{1}{2} \sum_{i=1}^m i n_i^2;$$

for if the feature values in class i are all distinct, the largest one exceeds $n_i - 1$ others, the second largest exceeds $n_i - 2$ others, and so on, and analogously in case of ties. We now show

the equality of the numerators in (3.8) and (3.11), in that

$$\begin{aligned}
& \sum_{i=1}^{m-1} \sum_{j=i+1}^m \sum_{k=1}^{n_i} \sum_{l=1}^{n_j} (j-i) s(x_{ik}, x_{jl}) \\
&= \sum_{i=1}^{m-1} \sum_{j=i+1}^m \sum_{k=1}^{n_i} \sum_{l=1}^{n_j} j s(x_{ik}, x_{jl}) - \sum_{i=1}^{m-1} \sum_{j=i+1}^m \sum_{k=1}^{n_i} \sum_{l=1}^{n_j} i s(x_{ik}, x_{jl}) \\
&\quad + \sum_{j=1}^{m-1} \sum_{i=j+1}^m \sum_{k=1}^{n_j} \sum_{l=1}^{n_i} j s(x_{ik}, x_{jl}) - \sum_{j=1}^{m-1} \sum_{i=j+1}^m \sum_{k=1}^{n_j} \sum_{l=1}^{n_i} j s(x_{ik}, x_{jl}) \\
&= \sum_{i=1}^m \sum_{\substack{j=1 \\ j \neq i}}^m \sum_{k=1}^{n_i} \sum_{l=1}^{n_j} j s(x_{ik}, x_{jl}) - \sum_{i=1}^{m-1} \sum_{j=i+1}^m \sum_{k=1}^{n_i} \sum_{l=1}^{n_j} i (s(x_{jl}, x_{ik}) + s(x_{ik}, x_{jl})) \\
&= \sum_{j=1}^m \sum_{l=1}^{n_j} j \left(\overline{\text{rk}}(x_{jl}) - \frac{1}{2} \right) - \sum_{i=1}^m \sum_{k=1}^{n_i} \sum_{l=1}^{n_i} i s(x_{il}, x_{ik}) - \sum_{i=1}^{m-1} \sum_{j=i+1}^m i n_i n_j \\
&= \sum_{i=1}^m \sum_{k=1}^{n_i} i \overline{\text{rk}}(x_{ik}) - \frac{1}{2} \sum_{i=1}^m i n_i - \frac{1}{2} \sum_{i=1}^m i n_i^2 - n \sum_{i=1}^{m-1} i n_i + \sum_{i=1}^{m-1} i n_i \sum_{j=0}^i n_j \\
&= \sum_{i=1}^m \sum_{k=1}^{n_i} i \overline{\text{rk}}(x_{ik}) - \frac{1}{2} \sum_{i=1}^m i n_i - \frac{1}{2} \sum_{i=1}^m i n_i^2 - n \sum_{i=1}^m i n_i + \sum_{i=1}^m i n_i \sum_{j=0}^i n_j \\
&= \sum_{i=1}^m \sum_{k=1}^{n_i} i \overline{\text{rk}}(x_{ik}) + \sum_{i=1}^m i n_i \left(\sum_{j=0}^{i-1} n_j + \frac{1}{2} n_i - n - \frac{1}{2} \right).
\end{aligned}$$

As for the denominators,

$$\begin{aligned}
& \sum_{i=1}^{m-1} \sum_{j=i+1}^m (j-i) n_i n_j \\
&= \sum_{i=1}^{m-1} \sum_{j=i+1}^m j n_i n_j - \sum_{i=1}^{m-1} \sum_{j=i+1}^m i n_i n_j \\
&= \sum_{i=1}^m i n_i \sum_{k=0}^{i-1} n_k - n \sum_{i=1}^{m-1} i n_i + \sum_{i=1}^{m-1} i n_i \sum_{k=1}^i n_k \\
&= 2 \sum_{i=1}^m i n_i \sum_{k=0}^{i-1} n_k - n \sum_{i=1}^{m-1} i n_i + \sum_{i=1}^{m-1} i n_i^2 + \sum_{i=1}^{m-1} i n_i \sum_{k=0}^{i-1} n_k - \sum_{i=1}^m i n_i \sum_{k=0}^{i-1} n_k \\
&= 2 \sum_{i=1}^m i n_i \sum_{k=0}^{i-1} n_k - n \sum_{i=1}^{m-1} i n_i + \sum_{i=1}^{m-1} i n_i^2 - n m n_m + m n_m^2
\end{aligned}$$

$$\begin{aligned}
&= 2 \sum_{i=1}^m i n_i \sum_{k=0}^{i-1} n_k - n \sum_{i=1}^m i n_i + \sum_{i=1}^m i n_i^2 \\
&= \sum_{i=1}^m i n_i \left(2 \sum_{j=0}^{i-1} n_j + n_i - n \right),
\end{aligned}$$

whence the proof is complete. \square

Interestingly, the representation (3.10) in terms of rank and class based covariances appears to be new even in the special case when the outcomes are binary, so that CPA reduces to AUC. The representation also sheds new light on the asymmetry of CPA, in that, in general, the value of CPA changes if we transpose the roles of the feature and the outcome. In stark contrast to customarily used measures of bivariate association and dependence, which are necessarily symmetric (22–23, 42), CPA is directed and aimed at quantifying predictive potential.

3.4.3 Relationship to Spearman’s rank correlation coefficient

Spearman’s rank correlation coefficient ρ_S for data of the form (3.1) is defined as Pearson’s correlation coefficient applied to the respective ranks (25). In case there are no ties in either x_1, \dots, x_n nor y_1, \dots, y_n , the concept is unambiguous, and Spearman’s coefficient can be computed as

$$\rho_S = 1 - \frac{6}{n(n^2 - 1)} \sum_{i=1}^n (\text{rk}(x_i) - \text{rk}(y_i))^2, \quad (3.12)$$

where $\text{rk}(x_i)$ denotes the rank of x_i within x_1, \dots, x_n , and $\text{rk}(y_i)$ the rank of y_i within y_1, \dots, y_n ,

In this setting CPA relates linearly to Spearman’s rank correlation coefficient ρ_S , in the very same way that AUC relates to Somers’ D in eq. (2.5).

Theorem 3.6. *In the case of no ties,*

$$\text{CPA} = \frac{1}{2} (\rho_S + 1). \quad (3.13)$$

Indeed, in case there are no ties, both mid ranks and classes reduce to ranks proper, and then (3.13) is readily identified as a special case of (3.10). Note that CPA becomes symmetric in this case, as its value remains unchanged if we transpose the roles of the feature and the outcome. Furthermore, if the joint distribution of a bivariate random vector (X, Y) is continuous, and we think of the data in (3.1) as a sample from the respective population, then, by applying Definition 3.3 and Theorem 3.6 in the large sample limit, and taking (3.5) into account, we (informally) obtain a population version of CPA, namely,

$$\text{CPA} = 6 \int_0^1 \alpha(1 - \alpha) \text{AUC}_\alpha \, d\alpha = \frac{1}{2} (\rho_S + 1), \quad (3.14)$$

Table 1: Population values of Pearson’s correlation coefficient r , Spearman’s rank correlation coefficient ρ_S and CPA for the features X, X', X'' relative to the real-valued outcome Y , where (Y, X, X', X'') is Gaussian with covariance matrix (2.6).

Feature	r	ρ_S	CPA
X	0.800	0.786	0.893
X'	0.500	0.483	0.741
X''	0.200	0.191	0.596

where AUC_α is the population version of AUC for $(X, \mathbb{1}\{Y \geq q_\alpha\})$, with q_α denoting the α -quantile of the marginal law of Y . We defer a rigorous derivation of (3.14) to future work and stress that, as both X and Y are continuous here, their roles can be interchanged.

Under the assumption of multivariate normality, the population version of Spearman’s ρ_S is related to Pearson’s correlation coefficient r as

$$\rho_S = \frac{6}{\pi} \arcsin \frac{r}{2}; \quad (3.15)$$

see, e.g., Kruskal (41). Returning to the example in Section 2.3, where (Y, X, X', X'') is jointly Gaussian with covariance matrix (2.6), Table 1 states, for each feature, the population values of Pearson’s correlation coefficient r , Spearman’s rank correlation coefficient ρ_S and CPA relative to the real-valued outcome Y , as derived from (3.14) and (3.15). In Fig. 6 the CPA values for the features appear along with the UROC curves in the final static screen, subsequent to the ROC movie. The empirical values show the expected approximate agreement with the population quantities in the table.

Suppose now that the values y_1, \dots, y_n of the outcomes are unique, whereas the feature values x_1, \dots, x_n might involve ties. Let $p \geq 0$ denote the number of tied groups within x_1, \dots, x_n . If $p = 0$ let $V = 0$. If $p \geq 1$, let v_j be the number of equal values in the j th group, for $j = 1, \dots, p$, and let

$$V = \frac{1}{12} \sum_{j=1}^p (v_j^3 - v_j).$$

Then Spearman’s *mid rank adjusted* coefficient ρ_M is defined as

$$\rho_M = 1 - \frac{6}{n(n^2 - 1)} \left(\sum_{i=1}^n (\overline{\text{rk}}(x_i) - \text{rk}(y_i))^2 + V \right), \quad (3.16)$$

where $\overline{\text{rk}}$ is the aforementioned mid rank. As shown by Woodbury (40), if one assigns all possible combinations of integer ranks within tied sets, computes Spearman’s ρ_S in (3.12) on every such combination and averages over the respective values, one obtains the formula for ρ_M in (3.16).

The following result reduces to the statement of Theorem 3.6 in the case $p = 0$ when there are no ties in x_1, \dots, x_n either.

Theorem 3.7. *In case there are no ties within y_1, \dots, y_n ,*

$$\text{CPA} = \frac{1}{2} (\rho_M + 1). \quad (3.17)$$

Proof. As noted, ρ_M arises from ρ_S if one assigns all possible combinations of integer ranks within tied sets, computes ρ_S on every such combination and averages over the respective values. In view of (3.11), if there are no ties in y_1, \dots, y_n , averaging $\frac{1}{2} (\rho_S + 1)$ over the combinations yields $\frac{1}{2} (\rho_M + 1)$, which equals CPA by (3.10). \square

The relationships (2.5), (3.13) and (3.17) constitute but special cases of the general, covariance based representation (3.10). In this light, CPA provides a unified way of quantifying potential predictive ability for the full gamut of dichotomous, categorical, mixed discrete-continuous and continuous types of outcomes. In particular, CPA bridges and generalizes AUC, Somers' D and Spearman's rank correlation coefficient, up to a common linear relationship.

3.5 Computational issues

We turn to a discussion of the computational costs of generalized ROC analysis for a dataset of the form (3.1) or (3.7) with n instances and $m \leq n$ classes.

It is well known that a traditional ROC curve can be generated from a dataset with n instances in $O(n \log n)$ operations (3, Algorithm 1). A ROC movie comprises $m - 1$ traditional ROC curves, so in a naive approach, ROC movies can be computed in $O(mn \log n)$ operations. However, our implementation takes advantage of recursive relations between consecutive component curves ROC_{i-1} and ROC_i . While a formal analysis will need to be left to future work, we believe that our algorithm has computational costs of $O(n \log n)$ operations only. For the vertical averaging of the component curves in the construction of UROC curves, we partition the unit interval into 1,000 equally sized subintervals.

Importantly, CPA can be computed in $O(n \log n)$ operations, without any need to invoke ROC analysis, by sorting x_1, \dots, x_n and y_1, \dots, y_n , computing the respective mid ranks and classes, and plugging into the rank based representation (3.11).

3.6 Summary

We summarize properties of ROC movies, UROC curves and CPA, starting with the trivial but critically important observation that they nest the notions of traditional ROC analysis. The labels of the subsequent statements are chosen such that they allow for immediate comparison with the key insights of classical ROC analysis, as have been stated in Section 2.4.

- (0) In the case of a binary outcome, both the ROC movie and the UROC curve reduce to the ROC curve, and CPA reduces to AUC.

- (1) ROC movies, the UROC curve and CPA are straightforward to compute and interpret, in the (rough) sense of *the larger the better*.
- (2) CPA attains values between 0 and 1 and relates linearly to the covariance between the class of the outcome and the mid rank of the feature, relative to the covariance between the class and the mid rank of the outcome. In particular, if the outcomes are pairwise distinct, then $\text{CPA} = \frac{1}{2}(\rho_M + 1)$, where ρ_M is Spearman’s mid rank adjusted coefficient (3.16). If the outcomes are binary, then $\text{CPA} = \frac{1}{2}(D + 1)$ in terms of Somers’ D . For a perfect feature, $\text{CPA} = 1$, $\rho_M = 1$ under pairwise distinct and $D = 1$ under binary outcomes. For a feature that is independent of the outcome, $\text{CPA} = \frac{1}{2}$, $\rho_M = 0$ under pairwise distinct and $D = 0$ under binary outcomes.
- (3) The numerical value of CPA admits an interpretation as a weighted probability of concordance for feature–outcome pairs, with weights that grow linearly in the class based distance between outcomes.
- (4) ROC movies, UROC curves and CPA are purely rank based and, therefore, invariant under strictly increasing transformations. Specifically, if $\phi : \mathbb{R} \rightarrow \mathbb{R}$ and $\psi : \mathbb{R} \rightarrow \mathbb{R}$ are strictly increasing, then the ROC movie, UROC curve and CPA computed from

$$(\phi(x_1), \psi(y_1)), \dots, (\phi(x_n), \psi(y_n)) \in \mathbb{R} \times \mathbb{R} \tag{3.18}$$

are the same as the ROC movie, UROC curve and CPA computed from the data in (3.1).

We iterate and emphasize that, as an immediate consequence of the final property, ROC movies, UROC curves and CPA assess the discrimination ability or *potential* predictive ability of a feature, marker or test. Markedly different techniques are called for if one seeks to assess a forecast’s *actual* value in a given applied problem (43–45).

4 Real data examples

We give further details for the real data examples in the main text.

4.1 Survival data example

Figures 1 and 3 in the main text serve to illustrate and contrast traditional ROC curves, ROC movies and UROC curves. They are based on a classical dataset from a Mayo Clinic trial on primary biliary cirrhosis (PBC), a chronic fatal disease of the liver, that was conducted between 1974 and 1984 (7). The data are provided by various R packages, such as `SMPracticals` and `survival`, and have been analyzed in textbooks (8, 46). The outcome of interest is survival time past entry into the study. Patients were randomly assigned to either a placebo or treatment with the drug D-penicillamine. However, extant analyses do not show treatment effects (7), and

so we follow previous practice and study treatment and placebo groups jointly. We consider two biochemical markers, namely, serum albumin and serum bilirubin concentration in mg/dl, for which higher and lower levels, respectively, are known to be indicative of earlier disease stage, thus supporting survival. Hence, for the purposes of ROC analysis we reverse the orientation of the serum bilirubin values.

Given our goal of illustration, we avoid complications and remove patient records with censored survival times,² to obtain a dataset with $n = 161$ patient records and $m = 156$ unique survival times. The traditional ROC curves in Fig. 1 are obtained by binarizing survival time at a threshold of 1462 days, which is the survival time in the data record that gets closest to four years. The ROC movies and UROC curves in Fig. 3 are generated directly from the survival times, without any need to artificially pick a threshold. Code for the replication of this illustration in the R language and environment (33) is available on GitHub (34).

4.2 Numerical weather prediction (NWP) example

Figure 4 in the main text studies and documents recent progress in numerical weather prediction (NWP), which has experienced tremendous advance over the past few decades (28–30). Specifically, we consider forecasts of surface (2-meter) temperature, (10-meter) wind speed and 24-hour precipitation accumulation at lead times from a single day (24 hours) to five days (120 hours) ahead from the high-resolution model operated by the European Centre for Medium-Range Weather Forecasts (ECMWF, 31). The forecasts are initialized at 00:00 UTC and available online at <https://confluence.ecmwf.int/display/TIGGE>. As observational reference we take the ERA5 reanalysis product (48), which is available for download at <https://cds.climate.copernicus.eu/cdsapp#!/dataset/reanalysis-era5-single-levels?tab=overview>. We use forecasts and observations from $279 \times 199 = 55,521$ model grid boxes of size $0.25^\circ \times 0.25^\circ$ each in a geographic region that covers Europe from 25.0° W to 44.5° E in latitude and 25.0° N to 74.5° N in longitude. The time period considered ranges from January 2007 to December 2018. Code for replication in the R language and environment (33) and Python (49) is available on GitHub (34).

Figure 8 is an extended version of Fig. 4 in the main text, in that the forecasts from ECMWF high-resolution run are now compared to a reference technique, namely, the persistence forecast. The persistence forecast is simply the most recent available observation for the weather quantity of interest; as such, it does not depend on the lead time. The CPA values are computed on rolling twelve-month periods that correspond to January–December, April–March, July–June or October–September, typically comprising $n = 365 \times 55,521 = 20,265,165$ individual forecast cases. The ECMWF forecast has considerably higher CPA than the persistence forecast for all lead times and variables considered. For the persistence forecast CPA fluctuates around a

²The proper handling of censoring is beyond the scope of our study, and we leave this task to subsequent work. For a discussion and comparison of extant approaches in the context of time-dependent ROC curves see Blanche et al. (47).

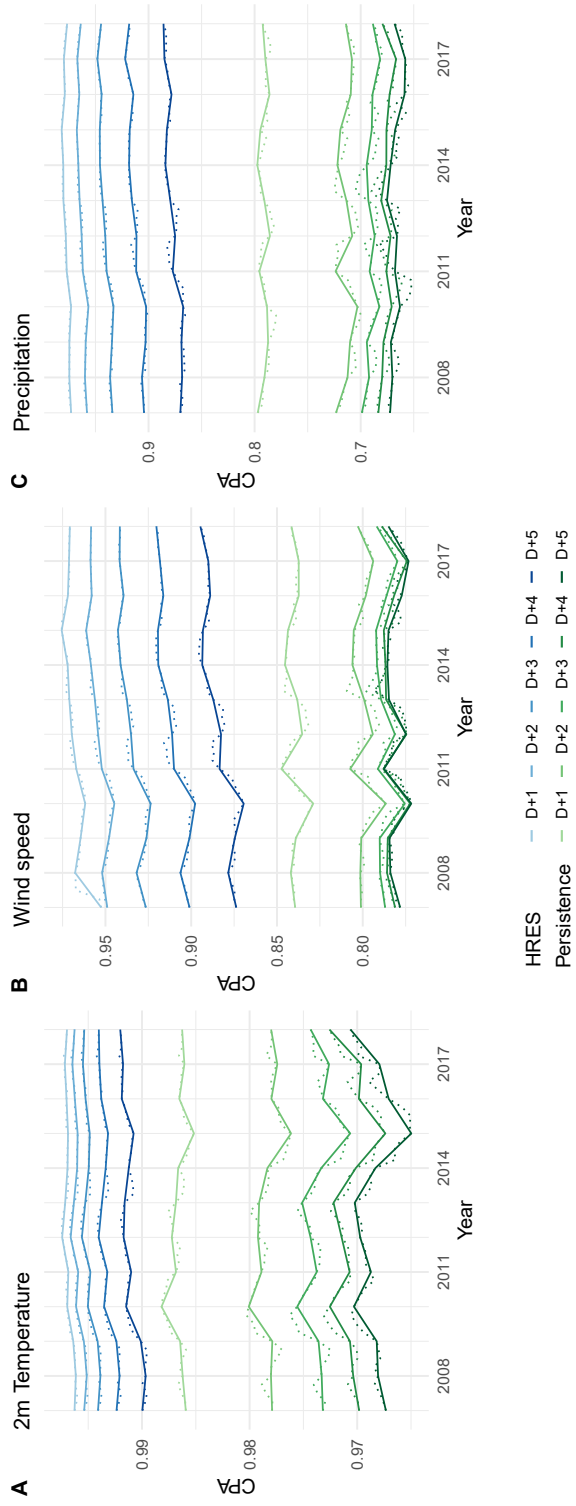


Figure 7: Same display as Fig. 4 in the main text, except that the forecasts from the ECMWF high-resolution run are compared to simplistic persistence forecasts. The CPA values refer to a domain that covers Europe and twelve-month periods that correspond to January–December (solid and dotted lines), April–March, July–June and October–September (dotted lines only), based on gridded forecast and observation data from January 2007 through December 2018.

Figure 8: ROC movies, UROC curves and CPA for ECMWF high-resolution (HRES) and persistence forecasts of 24-hour precipitation accumulation over Europe at a lead time of five days in calendar year 2018. In the ROC movies, the number at upper left shows the threshold at hand in the unit of millimeter, the number at upper center the relative weight $w_c / \max_{l=1, \dots, m-1} w_l$ from (3.4), and the numbers at bottom right the respective AUC values.

constant level; for the ECMWF forecast CPA improves steadily, attesting to continuing progress in NWP (28–30, 50).

To place these findings further into context, recall that CPA is a weighted average of AUC values for binarized outcomes at individual threshold values. Weightings other than in (3.4) are feasible, and relate to current practice for performance monitoring and headline scores at ECMWF, which involve AUC for binarized outcomes at a single threshold (30, 49), which obtains all of the weight, while the other thresholds get ignored. The new CPA measure preserves the spirit and power of classical ROC analysis, and frees researchers from the need to binarize real-valued outcomes.

The ROC movies, UROC curves and CPA values in Fig. 8 compare the ECMWF high-resolution forecast to the persistence forecast for 24-hour precipitation accumulation at a lead time of five days in calendar year 2018. As noted, this record comprises more than 20 million individual forecast cases, and there are $m = 35,993$ unique values of the outcome. Evidently, we lack the patience to watch the full sequence of $m-1$ screens in the ROC movie. A pragmatic solution is to consider a subset $C \subseteq \{1, \dots, m-1\}$ of indices, so that ROC_c is included in the ROC movie (if and) only if $c \in C$. Specifically, we set positive integer parameters $a \leq m-1$ and b such that the ROC movie comprises at least a and at most $a+b$ curves. Let the integer s

be defined such that $1 + (a - 1)s \leq m - 1 < 1 + as$, and let $C_a = \{1, 1 + s, \dots, 1 + (a - 1)s\}$, so that $|C_a| = a$. Let $C_b = \{c : n_c \geq n/b\}$; evidently, $|C_b| \leq b$. Finally, let $C = C_a \cup C_b$ so that $a \leq |C| \leq a + b$. We have made good experiences with choices of $a = 400$ and $b = 100$, which in Fig. 8 yield a ROC movie with 401 screens.

Additional references

35. D. J. Hand, Till, R. J., A simple generalization of the area under the ROC curve to multiple class classification problems. *Mach. Learn.* **45**, 171–186 (2001).
36. T. Gneiting, P. Vogel, <https://arxiv.org/abs/1809.04808> (2018).
37. Y. Xie, animation, an R package for creating animations and demonstrating statistical methods. *J. Statist. Softw.* **53** (2013).
38. F. E. Harrell Jr., K. L. Lee, D. B. Mark, Tutorials in biostatistics: Multivariable prognostic models: Issues in developing models, evaluating assumptions and adequacy, and measuring and reducing errors. *Stat. Med.* **15**, 361–387 (1996).
39. M. J. Pencina, R. B. D’Agostino, Evaluating discrimination of risk prediction models: The C statistic. *J. Am. Med. Assoc.* **314**, 1063–1064 (2015).
40. M. A. Woodbury, Rank correlation when there are equal variates. *Ann. Math. Statist.* **11**, 358–362 (1940).
41. W. H. Kruskal, Ordinal measures of association. *J. Am. Statist. Assoc.* **53**, 814–861 (1958).
42. J. Nešlehová, On rank correlation measures for non-continuous random variables. *J. Multivar. Anal.* **98**, 544–567 (2007).
43. T. Gneiting, Making and evaluating point forecasts. *J. Am. Stat. Assoc.* **106**, 746–762 (2010).
44. Z. Ben Bouallègue, P. Pinson, P. Friederichs, Quantile forecast discrimination and value. *Q. J. Roy. Meteorol. Soc.* **141**, 3415–3424 (2015).
45. W. Ehm, T. Gneiting, A. Jordan, F. Krüger, Of quantiles and expectiles: Consistent scoring functions, Choquet representations and forecast rankings (with discussion and rejoinder). *J. Roy. Stat. Soc. Ser. B* **78**, 505–562 (2016).
46. A. C. Davison. *Statistical Models* (Cambridge University Press, 2003).

47. P. Blanche, J.-F. Dartigues, H. Jacqmin-Gatta, Review and comparison of ROC curve estimators for a time-dependent outcome with marker-dependent censoring. *Biometr. J.* **55**, 687–704 (2013).
48. H. Hersbach *et al.*, Global reanalysis: Goodbye ERA-Interim, hello ERA5. *ECMWF Newsl.* **159**, 17–24 (2019).
49. Python Software Foundation, Python language reference, <http://www.python.org> (2019).
50. T. Haiden, M. Janousek, J. R. Bidlot, R. Buizza, L. Ferranti, F. Prates, F. Vitart, <https://www.ecmwf.int/en/elibrary/19277-evaluation-ecmwf-forecasts-including-2019-upgrade> (2019).